Journal of Hazardous Materials 163 (2009) 1101–1106

Contents lists available at ScienceDirect

Journal of Hazardous Materials

journal homepage: www.elsevier.com/locate/jhazmat

Reaction kinetics of photocatalytic degradation of sulfosalicylic acid using TiO_2 microspheres

Chuan Wang[a], Xianghua Zhang[b], Hong Liu[a,*], Xiangzhong Li[c], Wenzhao Li[b], Hengyong Xu[b]

[a] School of Chemistry and Chemical Engineering, Sun Yat-Sen University, Guangzhou 510275, China
[b] Dalian Institute of Chemical Physics, The Chinese Academy of Sciences, Dalian 116023, China
[c] Department of Civil and Structural Engineering, The Hong Kong Polytechnic University, Hung Hom, Kowloon, Hong Kong, China

ARTICLE INFO

Article history:
Received 20 March 2008
Received in revised form 26 June 2008
Accepted 16 July 2008
Available online 23 July 2008

Keywords:
Photocatalysis
Kinetics
Sulfosalicylic acid
TiO_2 microspheres

ABSTRACT

The photocatalytic (PC) degradation kinetics of sulfosalicylic acid (SSA) at different pH using TiO_2 microspheres were elucidated by modeling. The resultant model had special consideration of adsorption and pH. The adsorption isotherms showed that the LC/MS^2-identified intermediates were weakly adsorbed on the TiO_2 microspheres, thus their adsorption was neglected in the modeling. By contrast, the SSA was significantly adsorbed, thus its adsorption retained as an item in the model. Consequently, a non-first-order model was obtained. Through the modeling, it was elucidated that the reaction rate increased non-linearly with the SSA adsorption equilibrium constant. Meanwhile, it was elucidated that a pH increase favored the hydroxyl radical production to accelerate the SSA degradation, while impeded the SSA adsorption to slower it, hence a neutral pH caused the fastest SSA degradation.

1. Introduction

Photocatalytic (PC) reaction using TiO_2 to degrade biorefractory organic contaminants has a promising prospect in water treatment, and has been widely investigated in recent decades [1–6]. During this process, the highly active hydroxyl radicals (•OH) nonselectively attack the organic substrates to yield desired inorganic minerals.

For a best performance of the PC reaction, a variety of means including using modified TiO_2 [7–10], preparing novel TiO_2-based photocatalysts [11,12], and designing alternative reaction configurations [13–15] have been reported.

A photocatalyst different from the TiO_2 powders named TiO_2 microspheres has also been fabricated [16] for a best performance of the PC reaction. It has been established that the PC system with the microspheres ensures an efficient degradation of sulfosalicylic acid (SSA) and salicylic acid (SA). Moreover, the microspheres can be advantageously dispersed by air bubbling for efficient illumination, and can settle down to the reactor bottom quickly through gravity for a rapid separation from the aqueous phase once the air bubbling stops. It is claimed that the sufficiently robust microspheres not only take care of the illumination losses encountered in the immobilized PC system but also overcome the main drawback of TiO_2 separation faced by the suspended PC system [16].

Along with the performance evaluation, the kinetics of the substrate degradation are of profound interest for optimizing the PC system. Although the pseudo-first-order reaction model has been frequently employed to describe the degradation kinetics of PC reaction [17,18], it is not capable of fitting the degradation data of SSA and SA adequately in the TiO_2 microsphere PC system. Instead, a different reaction kinetic equation well fits the degradation data [16]. Such equation includes the item of adsorption, thus is more informative than the pseudo-first-order one that is oversimplified without any inclusion of the influencing factors. Obviously, the inclusion of vital factors in the kinetic model is of importance, because the factors such as adsorption influence the PC kinetics significantly [11,19–21], and understanding them helps one to evaluate the process efficiency and optimize the operating parameters.

More recently, a study continues to disclose the relationship between the adsorption and the degradation kinetics of SA at different pH [22], since the pH is another vital factor influencing the PC reaction significantly [2]. However, the kinetics, particularly the effects of adsorption and pH, have not been elucidated by modeling.

Accordingly, herein we extend the previous study by conducting the SSA degradation using the TiO_2 microspheres at different pH values, then focusing on elucidating the reaction kinetics through modeling on the basis of the generally accepted PC mechanism. The

* Corresponding author. Tel.: +86 2084115573; fax: +86 2084110927.
E-mail address: ceshliu@mail.sysu.edu.cn (H. Liu).

0304-3894/$ – see front matter © 2008 Elsevier B.V. All rights reserved.
doi:10.1016/j.jhazmat.2008.07.064

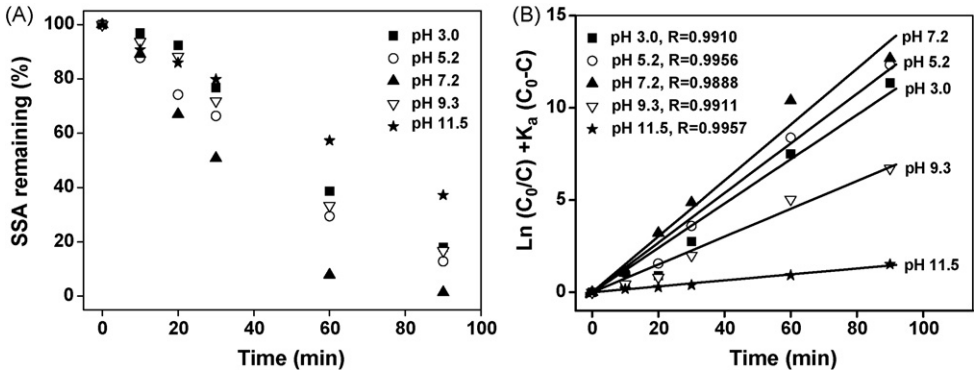

Fig. 1. SSA degradation at different pH (A) and the fitting results of the SSA degradation data by Eq. (1).

resultant model includes various factors, yet of them the adsorption and the pH are addressed.

2. Experimental methodology

2.1. Chemicals and instruments

The acetonitrile used for the present study was of HPLC grade and all the other chemicals were of analytical grade. Moreover doubly distilled water was used throughout the experiment. TiO_2 microspheres were prepared in accordance with a previously described method [16]. A Coulter (DELSA 440SX) Doppler electrophoretic light scattering analyzer was employed for the measurement of zeta potential. HPLC (Waters 486) equipped with a reverse phase column (Waters, XTerra™ MS C-18, 5 μm) and a UV detector was employed for the quantification of SSA concentrations. The composition of the mobile phase was acetonitrile and water, 40:60% for SSA, *p*-phenolsulfonic acid and benzenesulfonic acid, and 20:80% for phenol. The detection wavelength was 296 nm for SSA, 269 nm for phenol, 264 nm for *p*-phenolsulfonic acid, and 229 nm for benzenesulfonic acid. A liquid chromatography–Mass/Mass (LC/MS^2) system was employed for the identification of the intermediates of SSA degradation. The LC part consists of a gradient pump (Spectra System P4000), an autosampler (Spectra System Tem AS3000) with a 20 μL injection loop, a Thermo Ques Hypersil ODS column (C18, 5 μm, 250 mm × 4.6 mm ID) and a photodiode array UV detector (Spectra SYSTEM UV6000LP). The intermediates were determined by an ion trap mass spectrometer (Finnigan Duo LCQ MS/MS system) with either electrospray ionization probe or atmospheric pressure chemical ionization probe. Nitrogen gas was generated by a generator (NITROX) and used as both sheath and auxiliary gases.

2.2. Experimental procedure

Adsorption experiments of SSA and its degradation intermediates were performed in the dark by shaking 10.0 mL adsorbate with a known concentration and 0.20 g TiO_2 microspheres in a container at 130 r min^{-1} for 24 h at 25 °C. The zeta potential of TiO_2 microspheres was measured. Prior to measurement, the TiO_2 microspheres were suspended by an ultrasonic for 60 min in 0.01 M KNO_3 solution. The PC degradation of SSA was conducted in a cylindrical quartz reactor with an effective volume of 165 mL as described previously [16]. Briefly, in the reactor, 3.5 g L^{-1} TiO_2 microspheres were fully fluidized through air bubbling. A 6 W near UV lamp with a main emission at 365 nm illuminated the reactor. The illumination intensity was 2.0 mW cm^{-2} measured by a black-ray ultraviolet meter (Model No. J221, USA).

3. Results and discussion

3.1. PC degradation of SSA

Fig. 1 illustrates the PC degradation results of SSA using the TiO_2 microspheres at different pH values. Clearly, the PC degradation rate increased from pH 3.0 to 7.2, then decreased from pH 7.2 to 11.5, and the fastest degradation occurred at pH 7.2 while the slowest at pH 11.5. In the previous study [16], the pseudo-first-order reaction model was inadequate to fit the SSA degradation at pH 7.2, whereas, a different model was adequate to describe the SSA degradation at pH 7.2:

$$\ln\left(\frac{C_0}{C}\right) + K_a(C_0 - C) = K_{app}t \quad (1)$$

where K_a and K_{app} are adsorption equilibrium constant of SSA and apparent rate constant, respectively. In this work, the similar inadequacy was also encountered to fit the data in Fig. 1A by using the pseudo-first-order reaction model, whereas Eq. (1) fitted the SSA degradation data quite well (Fig. 1B).

3.2. Model development

As generally accepted, the PC reaction begins with a generation of electrons and holes (e–h pairs) upon irradiation by energy higher than the TiO_2 band gap [1]. The holes move to the TiO_2 surface and react with the water molecule to produce •OH radicals [23]. Also, the substrate adsorption on the TiO_2 microspheres should be considered since the microspheres are featured with a relatively large pore volume of 0.388 cm^3 g^{-1} and surface area of 1208 m^2 g^{-1} [16]. The adsorption/desorption equilibrium of the organic substrate on the TiO_2 microspheres can be expressed as:

$$\mathrm{Or} + \mathrm{TiO_2} \underset{k_{-1}}{\overset{k_{+1}}{\rightleftharpoons}} [\mathrm{Or} - \mathrm{TiO_2}]_{\mathrm{adsorb}} \quad (2)$$

where Or is the organic substrate and $[\mathrm{Or} - \mathrm{TiO_2}]_{\mathrm{adsorb}}$ is its adsorbed species, and the generation of e–h pairs can be expressed as:

$$\mathrm{TiO_2} + h\nu \underset{k_{-2}}{\overset{k_{+2}}{\rightleftharpoons}} \mathrm{e} + \mathrm{h} \quad (3)$$

Then, the production of •OH radicals can be written as follows:

$$h + \mathrm{H_2O} \underset{k_{-3}}{\overset{k_{+3}}{\rightleftharpoons}} {}^{\bullet}\mathrm{OH} + \mathrm{H^+} \quad (4)$$

where k_{+1}, k_{+2} and k_{+3} are rate constants of forward reactions, and k_{-1}, k_{-2} and k_{-3} of backward reactions. The •OH radicals attack the

adsorbed substrate to form intermediates P_i that are also adsorbed on the microspheres:

$$^{\bullet}OH + (Or - TiO_2)_{adsorb} \xrightarrow{k_4} P_i \quad (5)$$

$$P_i + TiO_2 \underset{k_{-i}}{\overset{k_{+i}}{\Leftrightarrow}} (P_i - TiO_2)_{adsorb} \quad (6)$$

where i is integer larger than 4, P_i is intermediate and $(P_i - TiO_2)_{absorb}$ is its adsorbed species. The $^{\bullet}OH$ radicals are active and transient [24], and there is no stable species of the adsorbed $^{\bullet}OH$. As a result, the organic degradation occurs between its adsorbed species and the $^{\bullet}OH$ radicals [25], and the kinetic equation describing the organic degradation can be written as:

$$-\frac{dC}{dt} = k_4 \tau [^{\bullet}OH]\theta_A \quad (7)$$

where C is the organic concentration, τ is the lifetime of $^{\bullet}OH$, $[^{\bullet}OH]$ is the concentration of $^{\bullet}OH$, θ_A is the coverage of organic substrate adsorbed on the TiO_2 surface, and k_4 is the rate constant.

The PC reaction experiment starts after the adsorption/desorption equilibrium is established, moreover, such equilibrium is considered to keep under the irradiation [26]. Hence, Eqs. (8) and (9) can be obtained from Eqs. (2) and (6), respectively:

$$k_{+1}C\left(1 - \theta_A - \sum_{i=5}^{n}\theta_i\right) - k_{-1}\theta_A = 0 \quad (8)$$

$$k_{+i}C_i\left(1 - \theta_A - \sum_{i=5}^{n}\theta_i\right) - k_{-i}\theta_i = 0 \quad (9)$$

where C_i is the concentration of P_i. Let $K_a = k_{+1}/k_{-1}$, and $K_i = k_{+1}/k_{-1}$, then a combination of Eqs. (8) and (9) yields the following equation:

$$\theta_A = \frac{K_a C}{1 + \sum_{i=5}^{n} K_i C_i + K_a C} \quad (10)$$

where K_a and K_i are the adsorption equilibrium constants of parent substrate and intermediate, respectively. Then, from Eq. (4), Eq. (11) can be obtained:

$$k_{+3}[h] = k_{-3}[^{\bullet}OH][H^+] \quad (11)$$

Then, $[^{\bullet}OH]$ can be expressed below:

$$[^{\bullet}OH] = \frac{k_{+3}[h]}{k_{-3}[H^+]} \quad (12)$$

A combination of Eqs. (7), (10) and (12) yields Eq. (13) as below:

$$-\frac{dC}{dt} = \frac{k_{+3}k_4\tau[h]}{k_{-3}[H^+]}\frac{K_a C}{1 + \sum_{i=5}^{n} K_i C_i + K_a C} \quad (13)$$

From Eq. (13), besides pH and adsorption (K_a and K_i), other factors such as the reaction constants, hole concentration, radical lifetime are included. Apparently, large values of k_{+3}, k_4, $[h]$, τ and K_a benefit the PC reaction, while large values of k_{-3}, K_i and $[H^+]$ impede the PC reaction.

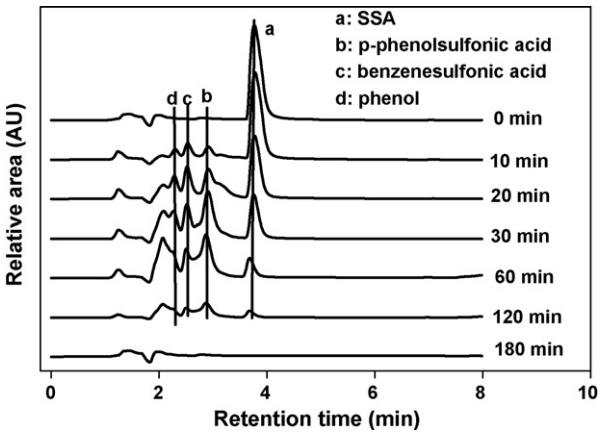

Fig. 2. LC diagram of the reacted solution during SSA degradation.

3.3. Neglection of intermediate adsorption in the modeling

Adsorption of the intermediates is included in Eq. (13). Since unstable intermediates occupy the active sites on the TiO_2 surface only transiently, the influence of the stable intermediates has only been considered. Identification of the intermediates during the PC degradation of SSA was performed by LC/MS^2 method. LC/MS is effective to identify the organic degradation intermediates [16]. The LC diagram of reacted solution at different time intervals is shown in Fig. 2, which indicated that some stable intermediates were involved in the PC reaction. Also, the MS results are listed in Table 1. Because the peaks at 2.28 and 2.52 min retention time had the same UV absorption, they were considered identical and no further differentiation was made. Consequently, by addition of the known compounds, three main stable intermediates were qualified as *p*-phenolsulfonic acid (peak a), benzenesulfonic acid (peak b) and phenol (peak c).

The adsorption experiments of the three intermediates on the TiO_2 microspheres were performed, and the results are shown in Fig. 3A. The data could be well fitted by the Langmuir adsorption model below:

$$\frac{C_e}{W} = \frac{1}{W_{sat}}C_e + \frac{1}{W_{sat}K_a} \quad (14)$$

where C_e is the equilibrium concentration of adsorbate, W and W_{sat} are the adsorption amount and saturated amount, respectively. The fitting results showed that the intermediates were weakly adsorbed because the K_i was as small as less than 1.0×10^3 L mol^{-1}. Also, the C_i was detected to be smaller than 5.0×10^{-5} M, and in the pH range of 3.0–11.0, the K_i was calculated to vary in the range of 8.0×10^2–2.0×10^3 L mol^{-1} from Fig. 3A. Thus, the value of $\sum_{i=5}^{n} K_i C_i$ is neglected compared to 1 in Eq. (13), so it can be simplified as:

$$-\frac{dC}{dt} = \frac{k_{+3}k_4\tau[h]}{k_{-3}[H^+]}\frac{K_a C}{1 + K_a C} \quad (15)$$

Table 1
The MS/MS data of the main fragments corresponding to the peaks a, b, c, d in Fig. 2

Peak no.	Retention time (min)	*m/z* (% abundance)		Molecular weight	UV-peaks (nm)	Compound
		MS	MS/MS			
a	3.77	218 (100)	166.2 (100), 174(89), 158 (45), 123 (15), 109 (14.4)	218	220, 235, 296	SSA
b	2.92	174 (100)	174.3 (100), 95.6 (92), 132.0(80), 78.6 (49)	174	200, 229	*p*-Phenolsulfonic acid
c	2.52	158 (100)	158 (100), 102(68), 93.2(58), 58.2 (33)	152.2	216, 264	Benzene sulfonic acid
d	2.08	94 (100)	93.2 (100)	94	210, 269	Phenol

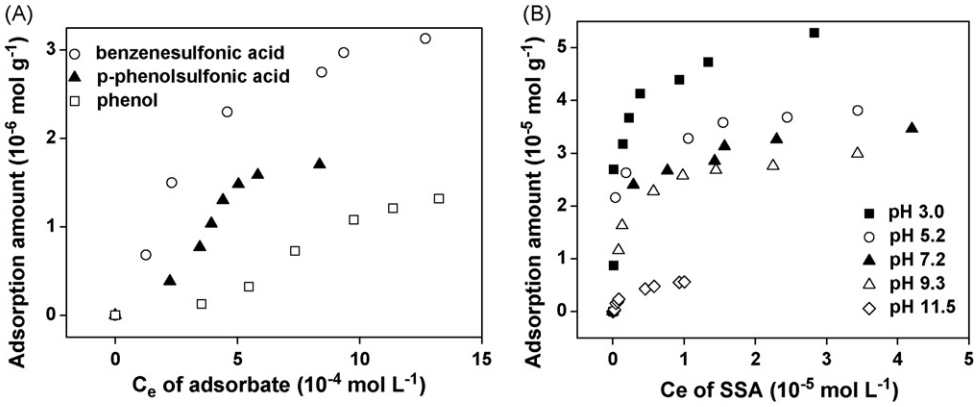

Fig. 3. Adsorption isotherms of the intermediates of SSA degradation at pH 7.2 (A) and of the SSA at different pH values (B) on TiO_2 microspheres.

3.4. Inclusion of SSA adsorption in the modeling

The adsorption of SSA retained as an item in Eq. (15). The adsorption experiments of SSA at different pH 3.0, 5.2, 7.2, 9.3, 11.5 were conducted using the TiO_2 microspheres. The results are illustrated in Fig. 3B, in which the data could be well fitted by the Langmuir adsorption model, and the fitted K_a values were 10.69×10^4, 10.15×10^4, 8.51×10^4, 5.92×10^4 and 0.85×10^4 L mol^{-1}. Also, the initial concentration was 1.0×10^{-4} mol L^{-1}, so the value of K_aC in Eq. (15) could not be neglected compared to 1. Thus, the model can be obtained by integrating Eq. (15):

$$\ln\left(\frac{C_0}{C}\right) + K_a(C_0 - C) = \frac{k_{+3}k_4\tau[h]}{k_{-3}[H^+]}K_a t \quad (16)$$

The $[H^+]$ variation during the PC reaction of SSA was neglected because <0.5 pH unit was detected before and after the PC reaction. Thus,

$$k_{app} = \frac{k_{+3}k_4\tau[h]}{k_{-3}[H^+]}K_a = k_r K_a \quad (17)$$

Then Eq. (18) identical to Eq. (1) is obtained:

$$\ln\left(\frac{C_0}{C}\right) + K_a(C_0 - C) = k_{app}t \quad (18)$$

As a result, a non-first-order reaction model to well fit the degradation of SSA at different pH (Fig. 1B) is obtained.

3.5. Effect of adsorption on the PC reaction

In Eq. (18), the K_a represented the adsorption. The relationship between the $-(dC/dt)$ and the K_a appears to be complicated and three cases exist. In case I, the value of K_aC is small, e.g., ≤0.1, so is neglected compared to 1. In this case, the $-(dC/dt)$ increases linearly with the K_a. Consequently, an integration of Eq. (15) yields the conventionally pseudo-first-order reaction model, applicable to describe the degradation kinetics of substrate with weak adsorption as below:

$$\ln\left(\frac{C_0}{C}\right) = k_{app}t \quad (19)$$

In case II, the value of K_aC, e.g., from 0.1 to 10, cannot be neglected compared to 1. In this case, the $-(dC/dt)$ increases with the K_a nonlinearly as simulated in Fig. 4. Thus, an integration of Eq. (15) yields Eq. (18), applicable to describe the degradation kinetics of substrate with a medium adsorption. The SSA degradation in Fig. 1 matched this case.

In case III, the value of K_aC, e.g., >10, is much larger than 1 and the item of 1 can be neglected. In this case, the $-(dC/dt)$ is independent on the K_a value, and the adsorption does not influence the PC degradation rate remarkably. Thus, an integration of Eq. (13) yields a zeroth-order reaction model, applicable to describe the degradation kinetics of substrate with strong adsorption as below:

$$\ln\left(\frac{C_0}{C}\right) = k_{app} \quad (20)$$

As for the PC system with SSA and TiO_2 microspheres, it has a particularity: the SSA shows a medium adsorption on the TiO_2 microspheres and the item designating the adsorption cannot be neglected in the kinetic model. Thus, a non-first-order kinetic model fits the SSA degradation quite well. It should be noted that the PC degradation of other substrates with weak and strong adsorption on the TiO_2 microspheres is rationally expected to obey the first-order and zeroth-order reaction model, respectively.

Under the condition of weak adsorption, even if the item designating the adsorption is neglected, the adsorption still influences the PC degradation linearly. Also, under the medium adsorption, the adsorption influences the PC degradation non-linearly. Only under the condition of strong adsorption, the PC degradation independent of the adsorption. Thus, it appears that when the adsorption is strong, the adsorption becomes a non-rate-determining step [27] and exhibits no effect on the PC reaction. In this case, any effort to accelerating the PC reaction by improving the adsorption appears to be in vain.

Interesting, the relationship between the reaction rate and the adsorption determines the format of the kinetic model. When the

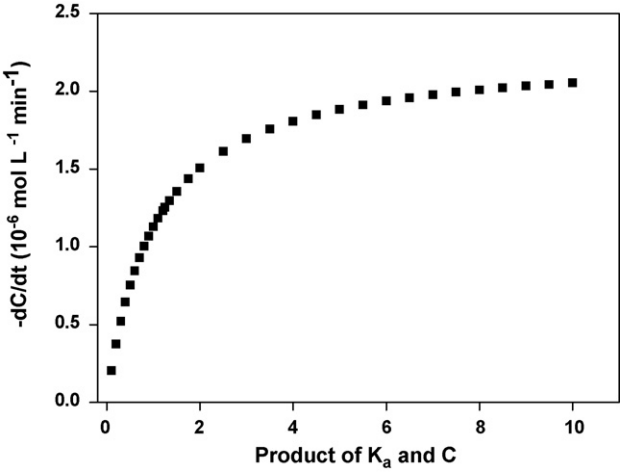

Fig. 4. Simulated relationship between $-(dC/dt)$ and K_aC with K_aC value from 0.1 to 10, and $((k_{+3}k_4\tau[h])/(k_{-3}[H^+]))$ 2.24×10^{-6} mol L^{-1} min^{-1}.

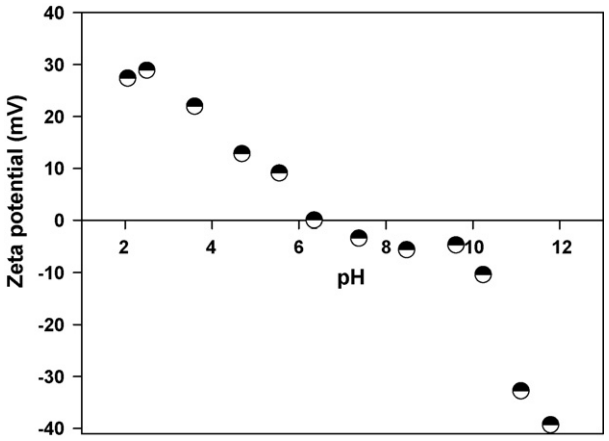

Fig. 5. Zeta potentials of the TiO_2 microspheres at different pH values.

reaction rate varies linearly with the adsorption, the kinetic model is correspondingly a first-order one (case I). When the reaction rate varies non-linearly with the adsorption, the kinetic model is a non-first-order one (case II). When the reaction rate does not vary with the adsorption, the kinetic model is a zeroth-order one (case III).

3.6. Effect of pH on the PC reaction

Also in Eq. (18), the k_r $((k_{+3}k_4\tau[h])/(k_{-3}[H^+]))$ rich in information represents the property of the reaction system. Obviously, the $-(dC/dt)$ increases linearly with the k_r that is determined by various factors of k_{+3}/k_{-3}, k_4, τ, $[h]$ and pH ($[H^+]$). Herein only the pH is addressed.

A high pH enhances the SSA degradation rate as can be seen from Eq. (15), and Eq. (12) shows that when a high pH helps to produce more •OH radicals since the OH^- is considered as the source of •OH. [28]. Therefore, a higher pH value benefits the SSA degradation via favoring the •OH production.

On the other hand, the pH influences the SSA degradation by influencing the adsorption [29]. When the pH value is smaller than the zero point of charge (ZPC) that has been measured to be 6.3 (Fig. 5), the surface charge of TiO_2 microspheres is positive. Yet, when the pH value overpasses the ZPC, the surface charge is negative. Meanwhile, the charge of organic substrate is negative due to dissociation. Therefore, a lower pH than the ZPC benefits the SSA degradation via favoring its adsorption.

From the above two aspects, it can be seen that the pH influences the PC reaction kinetics from two opposite treads to form a combined effect. Further, this combined effect can be understood more readily by means of Eq. (21) rewritten from Eq. (15):

$$-\frac{dC}{dt} = \frac{k_{+3}k_4\tau[h]}{k_{-3}[H^+]}\frac{C}{(1/K_a)+C} \quad (21)$$

Eq. (21) shows that a higher pH increases the PC reaction rate, whereas at the same time causes a smaller K_a value as earlier noted, so decreases the PC reaction rate. This combined effect leads to an increase in the PC reaction rate from pH 3.0 to 7.2, while a decrease from pH 7.2 to 11.5. Consequently, the fastest SSA degradation occurs at the neutral pH 7.2 (Fig. 1).

4. Conclusion

The established kinetic model enriches in the affecting factors such as adsorption of intermediates, adsorption of parent substrate and pH. Through the modeling, the effects of SSA adsorption and pH on the PC reaction kinetics can be well elucidated. The medium adsorption of SSA on the TiO_2 microspheres determines the format of the non-first-order model to well fit its PC degradation reaction, and influences the reaction rate non-linearly. Neutral pH causes the fastest degradation of SSA due to a combined effect of pH on the kinetics. This study provides an insight into and highlights the effects of adsorption and pH on the PC reaction.

Acknowledgements

This work is financially supported by the Natural Science Foundation of China (20207008), the RGC grant of Hong Kong Government (PolyU5148/03E) and the Innovative Project of Science &Technology, Guangzhou (055Z205005).

References

[1] F.B. Li, X.Z. Li, C.H. Ao, S.C. Lee, M.F. Hou, Enhanced photocatalytic degradation of VOCs using Ln–TiO_2 catalysts for indoor air purification, Chemosphere 59 (2005) 787–800.
[2] J.M. Herrmann, Heterogeneous photocatalysis: fundamentals and applications to the removal of various types of aqueous pollutants, Catal. Today 53 (1999) 115–129.
[3] K. Kabra, R. Chaudhary, R.L. Sawhney, Treatment of hazardous organic and inorganic compounds through aqueous-phase photocatalysis: a review, Ind. Eng. Chem. Res. 43 (2004) 7683–7696.
[4] C. McCullagh, J.M.C. Robertson, D.W. Bahnemann, P.K.J. Robertson, The application of TiO_2 photocatalysis for disinfection of water contaminated with pathogenic micro-organisms: a review, Res. Chem. Intermed. 33 (2007) 359–375.
[5] H. Sayılkan, Improved photocatalytic activity of Sn^{4+}-doped and undoped TiO_2 thin film coated stainless steel under UV- and vis-irradiation, Appl. Catal. A: Gen. 319 (2007) 230–236.
[6] J.G. Yu, G.H. Wang, B. Chen, M.H. Zhou, Effects of hydrothermal temperature and time on the photocatalytic activity and microstructures of bimodal mesoporous TiO_2 powders, Appl. Catal. B: Environ. 69 (2007) 171–180.
[7] H. Kato, A. Kudo, Visible-light-response and photocatalytic activities of TiO_2 and $SrTiO_3$ photocatalysts codoped with antimony and chromium, J. Phys. Chem. B 106 (2002) 5029–5034.
[8] W. Zhao, C.C. Chen, X.Z. Li, J.C. Zhao, H. Hidaka, N. Serpone, Photodegradation of sulforhodamine-B dye in platinized titania dispersions under visible light irradiation: influence of platinum as a functional co-catalyst, J. Phys. Chem. B 106 (2002) 5022–5028.
[9] H. Irie, Y. Watanabe, K. Hashimoto, Nitrogen-concentration dependence on photocatalytic activity of $TiO_{2-x}N_x$ powders, J. Phys. Chem. B 107 (2003) 5483–5486.
[10] C. Hu, X. Hu, L. Wang, J. Qu, A. Wang, Visible-light-induced photocatalytic degradation of azo dyes in aqueous AgI/TiO_2 dispersion, Environ. Sci. Technol. 40 (2006) 7903–7907.
[11] H. Liu, S.A. Cheng, J.Q. Zhang, C.N. Cao, S.K. Zhang, Titanium dioxide as photocatalyst on porous nickel: adsorption and the photocatalytic degradation of sulfosalicylic acid, Chemosphere 38 (1999) 283–292.
[12] H.Y. Zhu, X.P. Gao, Y. Lan, D.Y. Song, Y.X. Xi, J.C. Zhao, Hydrogen titanate nanofibers covered with anatase nanocrystals: a delicate structure achieved by the wet chemistry reaction of the titanate nanofibers, J. Am. Chem. Soc. 126 (2004) 8380–8381.
[13] M.A. Behnajady, N. Modirshahla, N. Daneshvar, M. Rabbani, Photocatalytic degradation of an azo dye in a tubular continuous-flow photoreactor with immobilized TiO_2 on glass plates, Chem. Eng. J. 127 (2007) 167–176.
[14] J.A. Byrne, B.R. Eggins, N.M.D. Brown, B. McKinney, M. Rouse, Immobilisation of TiO_2 powder for the treatment of polluted water, Appl. Catal. B: Environ. 17 (1998) 25–36.
[15] R. Dillert, A.E. Cassano, R. Goslich, D.W. Bahnemann, Large scale studies in solar catalytic wastewater treatment, Catal. Today 54 (1999) 267–282.
[16] X.Z. Li, H. Liu, L.F. Cheng, H.J. Tong, Photocatalytic oxidation using a new catalyst-TiO_2 microsphere-for water and wastewater treatment, Environ. Sci. Technol. 37 (2003) 3989–3994.
[17] K. Lv, Y. Xu, Effects of polyoxometalate and fluoride on adsorption and photocatalytic degradation of organic dye X_3B on TiO_2: the difference in the production of reactive species, J. Phys. Chem. B 110 (2006) 6204–6212.
[18] B. Toepfer, A. Gora, G.L. Puma, Photocatalytic oxidation of multicomponent solutions of herbicides: reaction kinetics analysis with explicit photon absorption effects, Appl. Catal. B: Environ. 68 (2006) 171–180.
[19] F. Zhang, J. Zhao, T. Shen, H. Hidaka, E. Pelizzetti, N. Serpone, TiO_2-assisted photodegradation of dye pollutants. II. Adsorption and degradation kinetics of eosin in TiO_2 dispersions under visible light irradiation, Appl. Catal. B: Environ. 15 (1998) 147–156.
[20] K.T. Ranjit, I. Willner, S.H. Bossmann, A.M. Braun, Lanthanide oxide doped titanium dioxide photocatalysts: effective photocatalysts for the enhanced degradation of salicylic acid and *t*-cinnamic acid, J. Catal. 204 (2001) 305–313.

[21] T. Sauer, G.C. Neto, H.J. Jose, R.F.P.M. Moreira, Kinetics of photocatalytic degradation of reactive dyes in a TiO_2 slurry reactor, J. Photochem. Photobiol. A: Chem. 149 (2002) 147–154.
[22] X.Z. Li, H. Liu, L.F. Cheng, H.J. Tong, Kinetic behavior of the adsorption and photocatalytic degradation of salicylic acid in aqueous TiO_2 microsphere suspension, J. Chem. Biotechnol. 79 (2004) 774–781.
[23] K. Rajeshwar, Photoelectrochemistry and the environment, J. Appl. Electrochem. 25 (1995) 1067–1082.
[24] Q.Q. Wang, A.T. Lemley, Kinetic model and optimization of 2,4-D degradation by anodic Fenton treatment, Environ. Sci. Technol. 35 (2001) 4509–4514.
[25] C.S. Turchi, D.F. Ollis, Photocatalytic degradation of organic water contaminants: mechanisms involving hydroxyl radical attack, J. Catal. 122 (1990) 178–192.
[26] Y. Xu, C.H. Langford, Variation of Langmuir adsorption constant determined for TiO_2-photocatalyzed degradation of acetophenone under different light intensity, J. Photochem. Photobiol. A: Chem. 133 (2000) 67–71.
[27] H. Liu, X.Z. Li, Y.J. Leng, W.Z. Li, An alternative approach to ascertain the rate-determining steps of TiO_2 photoelectrocatalytic reaction by electrochemical impedance spectroscopy, J. Phys. Chem. B 107 (2003) 8988–8996.
[28] M.C. Lu, G.D. Roam, J.N. Chen, C.P. Huang, Factors affecting the photocatalytic degradation of dichlorvos over titanium dioxide supported on glass, J. Photochem. Photobiol. A: Chem. 76 (1993) 103–110.
[29] C. Kormann, D.W. Bahnemann, M.R. Hoffmann, Photolysis of chloroform and other organic molecules in aqueous titanium dioxide suspensions, Environ. Sci. Technol. 25 (1991) 494–500.